PHYS 580 - Computational Physics

Computational Physics by *Nicholas J. Giordano, Hisao Nakanishi*

Student: **Ralph Razzouk**

Lab 4

Problem 1

Modify the provided starter code (pendulumRK2.m) (or write your own using any appropriate approximation) to study the Poincare section of the phase portrait and those of the time evolution of the dynamical variables θ, ω, and E (energy). Consider both $\theta - \omega$ and ω - E pairings (2D). Produce the Poincare sections for some model parameters in the normal periodic (with period $T = 2\pi/\Omega$, where Ω is the driving force angular frequency), chaotic, and period doubling (with period $2T$) regimes, choosing the sectioning and driving frequencies to be the same in all cases. Set the sectioning phase to 0 (i.e., do in phase sectioning). What are the characteristics of the different regimes reflected in these results? Explain how you can be sure that your computational parameters are sufficient to reach your conclusions.

Solution. For this problem, we consider the equations of motion for a driven damped pendulum with driving force F_D and driving frequency Ω_D:

$$\frac{\mathrm{d}\theta}{\mathrm{d}t} = \omega$$
$$\frac{\mathrm{d}\omega}{\mathrm{d}t} = -\omega_0^2 \sin\theta - q\omega + F_D \sin(\Omega_D t),$$

where $\omega_0 = \sqrt{g/L}$ is the natural frequency of the pendulum, q is the damping coefficient, and L is its length. We solve this system numerically using the Euler-Cromer method and considered three different regimes by varying the driving force F_D.

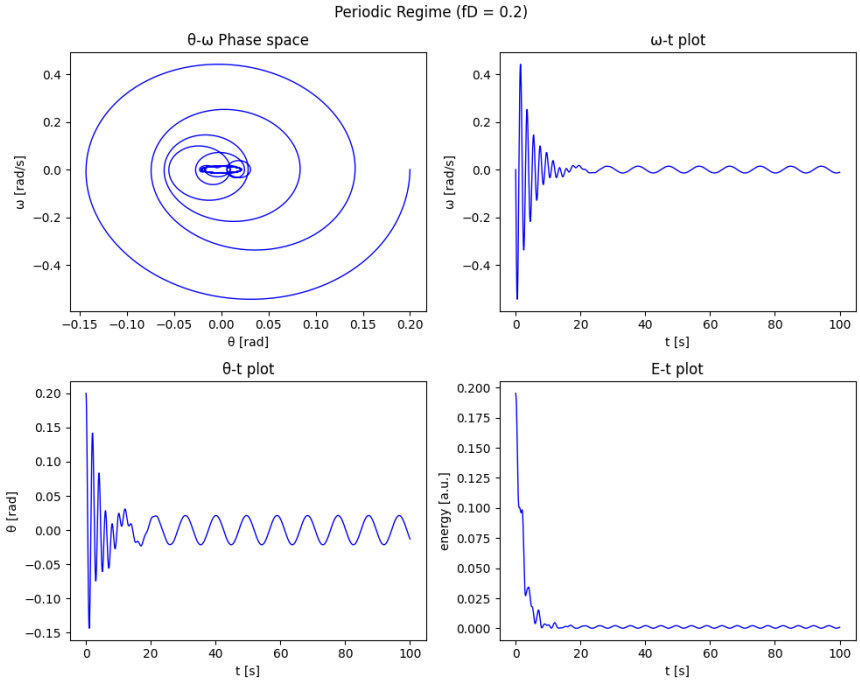

Figure 1: Plots of the phase spaces for the periodic regime.

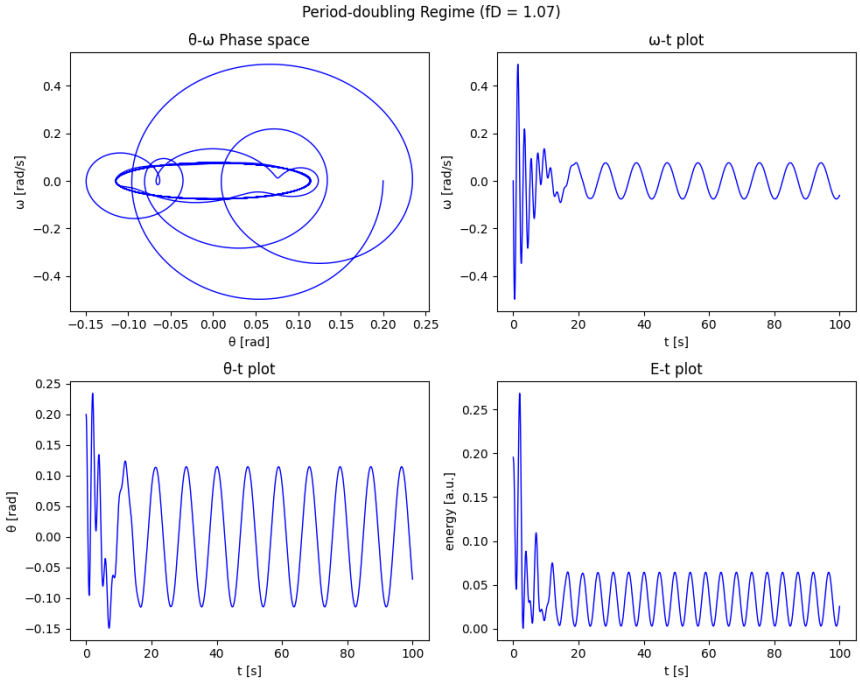

Figure 2: Plots of the phase spaces for the period-doubling regime.

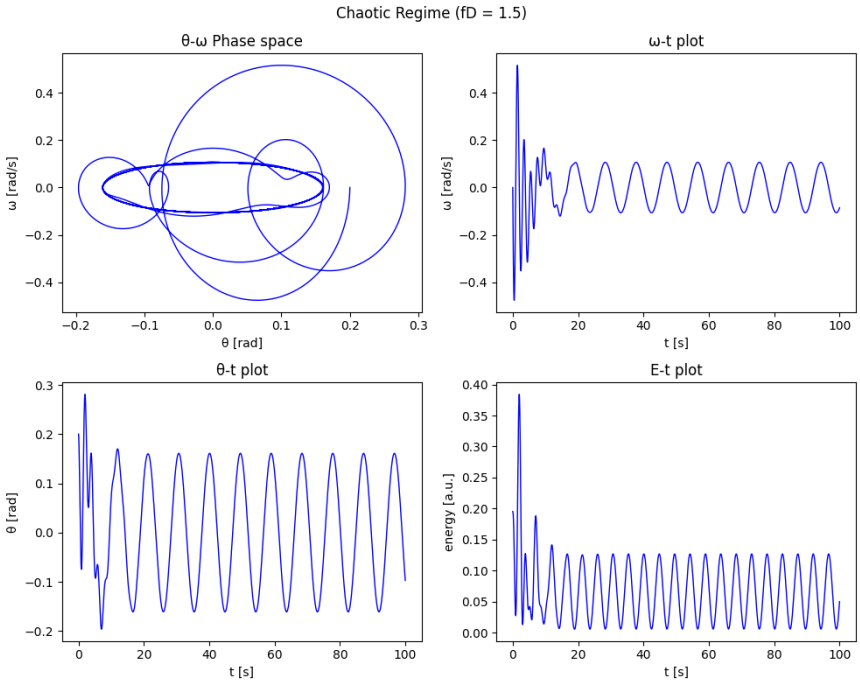

Figure 3: Plots of the phase spaces for the chaotic regime.

First, we consider a small driving force of $F_D = 0.2$. After the initial transient oscillations decay, we observe that the pendulum settles into a stable periodic motion. This can be seen in the phase space plot where the trajectory spirals inward to a single closed curve. The energy plot shows an initial rapid decrease due to

damping, followed by a constant amplitude oscillation once the pendulum reaches its steady state.
When we increase the driving force to $F_D = 1.07$, we enter a period-doubling regime. The phase space shows a more complex structure with the trajectory forming two interleaved orbits. This is reflected in the time evolution of θ and ω, where the amplitude of oscillation alternates between two values. The energy plot shows a similar pattern, oscillating between two distinct levels.
Finally, for $F_D = 1.5$, we enter the chaotic regime. The phase space shows a complex pattern that never exactly repeats. Both θ and ω exhibit irregular oscillations, and the energy varies in an apparently random manner, though still bounded. This behavior is characteristic of deterministic chaos, where the system remains bounded but shows extreme sensitivity to initial conditions.

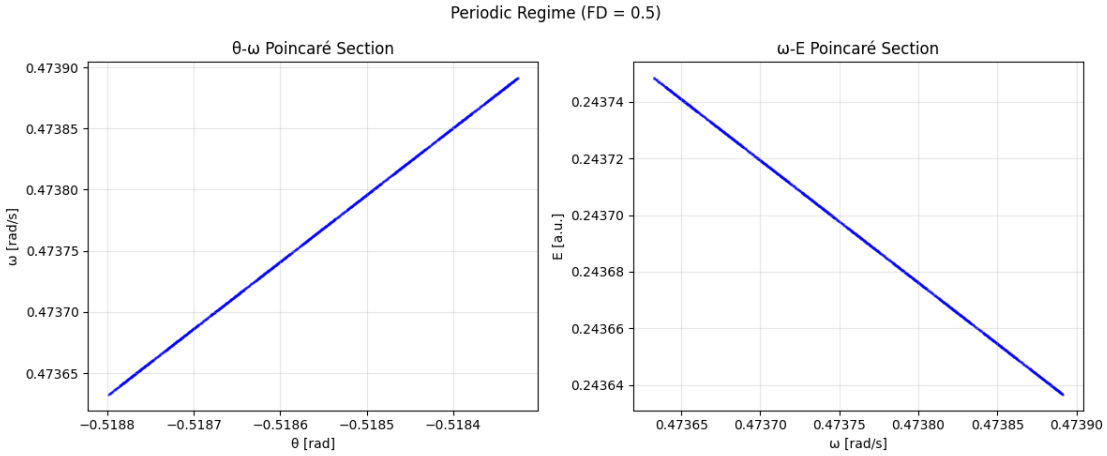

Figure 4: Plots of the phase spaces for the periodic regime.

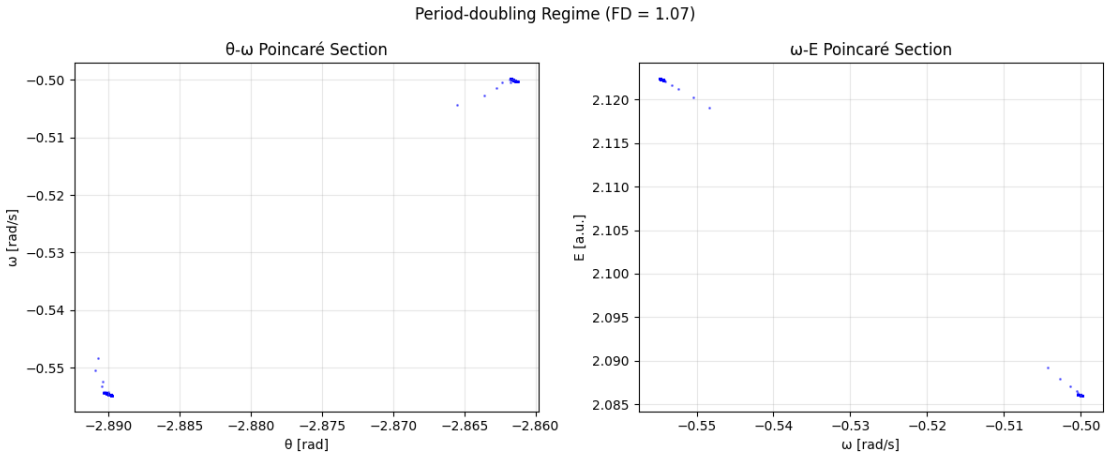

Figure 5: Plots of the phase spaces for the period-doubling regime.

To better understand these regimes, we also computed their Poincare sections by sampling the system's state at intervals of the driving period. For the periodic regime ($F_D = 0.5$), the Poincare section shows a single point in both θ-ω and ω-E spaces, confirming that the motion repeats exactly with the driving period. In the period-doubling regime ($F_D = 1.07$), we see two distinct points, indicating that the system takes two driving periods to complete one full cycle. For the chaotic regime ($F_D = 1.2$), the Poincare sections reveal a complex structure with points forming a strange attractor, characteristic of chaotic dynamics.
These results demonstrate how increasing the driving force can lead to increasingly complex behavior, from simple periodic motion to chaos, even in this relatively simple mechanical system. ■

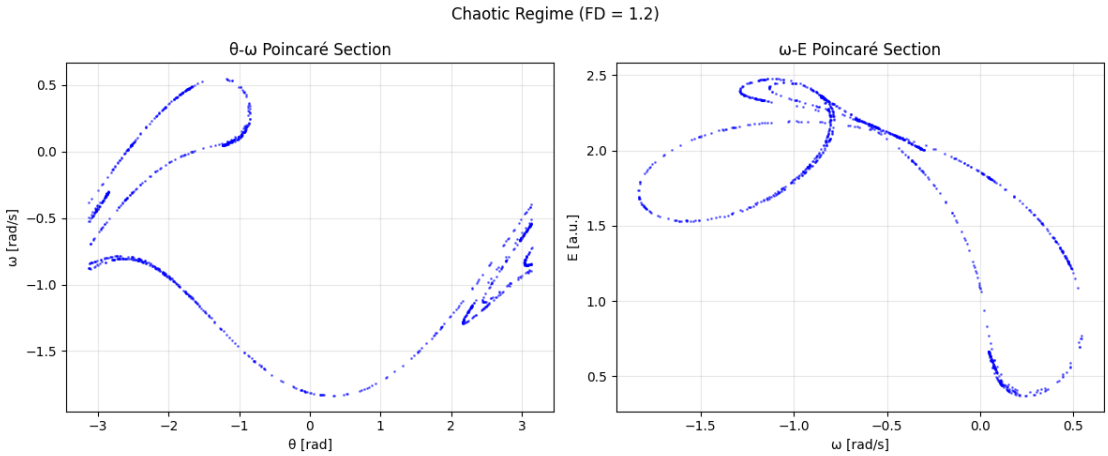

Figure 6: Plots of the phase spaces for the chaotic regime.

Problem 2
Second, investigate the effects, if any, of using different initial conditions $\theta(0)$ and $\omega(0)$, while keeping all other parameters the same as in (1). Explicitly compare results with those of part (1).

Solution. For this problem, we investigated how different initial conditions affect the pendulum's behavior in each regime while keeping all other parameters constant. We considered four different initial conditions:

$$(\theta_0, \omega_0) = (0.2, 0.0) \quad \text{(Original)}$$
$$(\theta_0, \omega_0) = (1.0, 0.0) \quad \text{(Larger angle)}$$
$$(\theta_0, \omega_0) = (0.2, 1.0) \quad \text{(Non-zero velocity)}$$
$$(\theta_0, \omega_0) = (-0.5, -0.5) \quad \text{(Different quadrant)}.$$

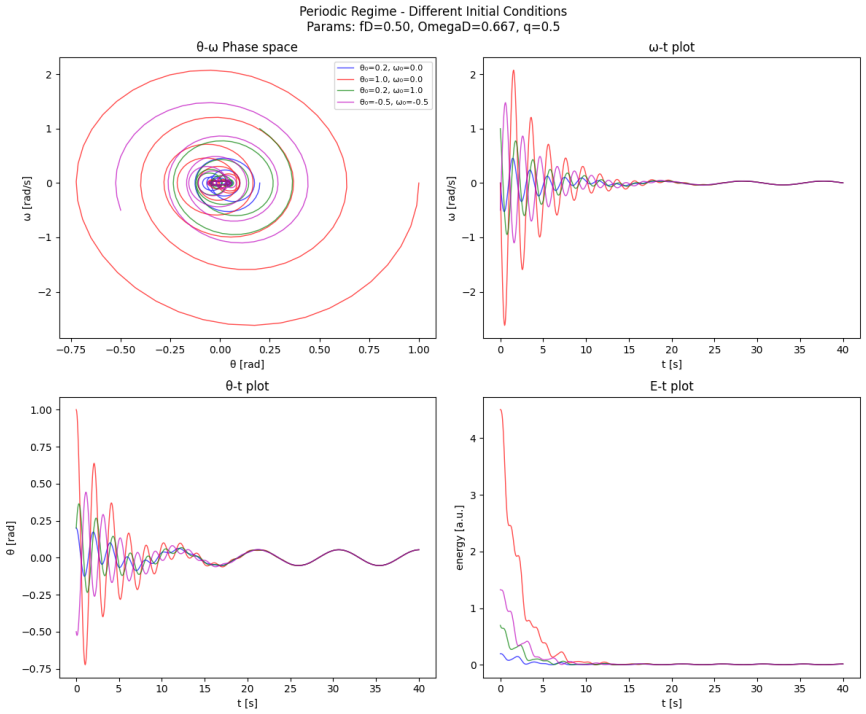

Figure 7: Plots of the phase spaces for the periodic regime with varied initial conditions.

For the periodic regime ($F_D = 0.5$), we observe that regardless of the initial conditions, all trajectories eventually converge to the same periodic orbit. This is evident in the phase space plot where all paths spiral inward to the same closed curve. The time evolution plots show different initial transients, but after these decay (around $t \approx 15$ s), all solutions oscillate with the same amplitude and phase. This behavior is characteristic of dissipative systems with a single stable attractor.
This convergence is even more clearly demonstrated in the Poincar sections. For the periodic regime, all initial conditions lead to the same single point in the section, confirming that the system has a unique stable periodic orbit. The ω-E Poincar section similarly shows convergence to a single point, indicating that the system settles into oscillations with a fixed energy.
In the period-doubling regime ($F_D = 1.07$), the convergence to the final state takes longer, but all trajectories still eventually settle into the same period-doubled oscillation. The phase space shows more complex initial paths before reaching the same double-loop structure. The Poincar sections reveal two distinct points regardless of initial conditions, confirming that all trajectories eventually exhibit the same period-doubling behavior.
For the chaotic regime ($F_D = 1.2$), while different initial conditions lead to different initial paths, they all explore similar regions of phase space after the transients decay. The Poincar sections show that all

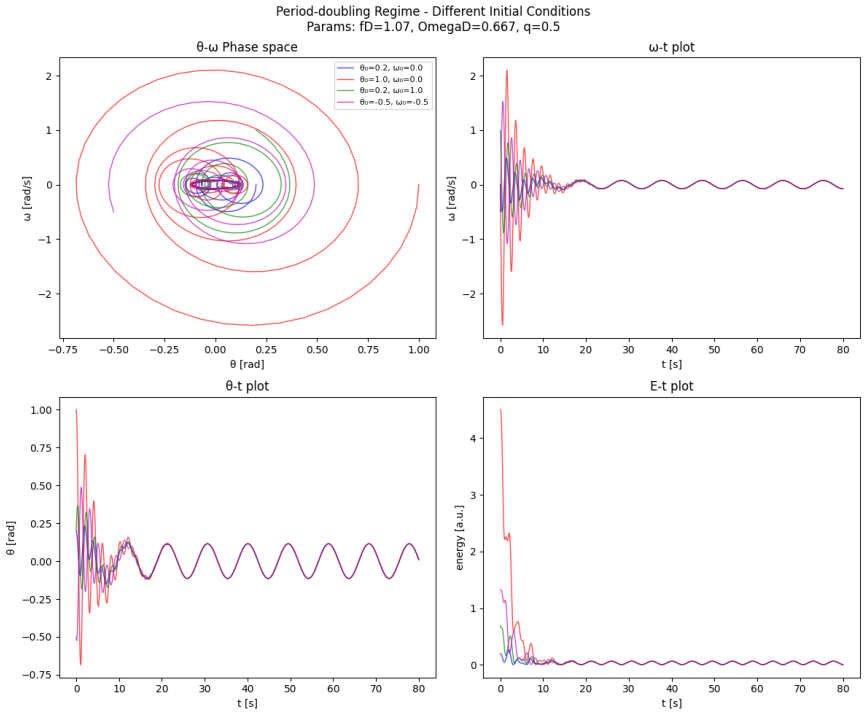

Figure 8: Plots of the phase spaces for the period-doubling regime with varied initial conditions.

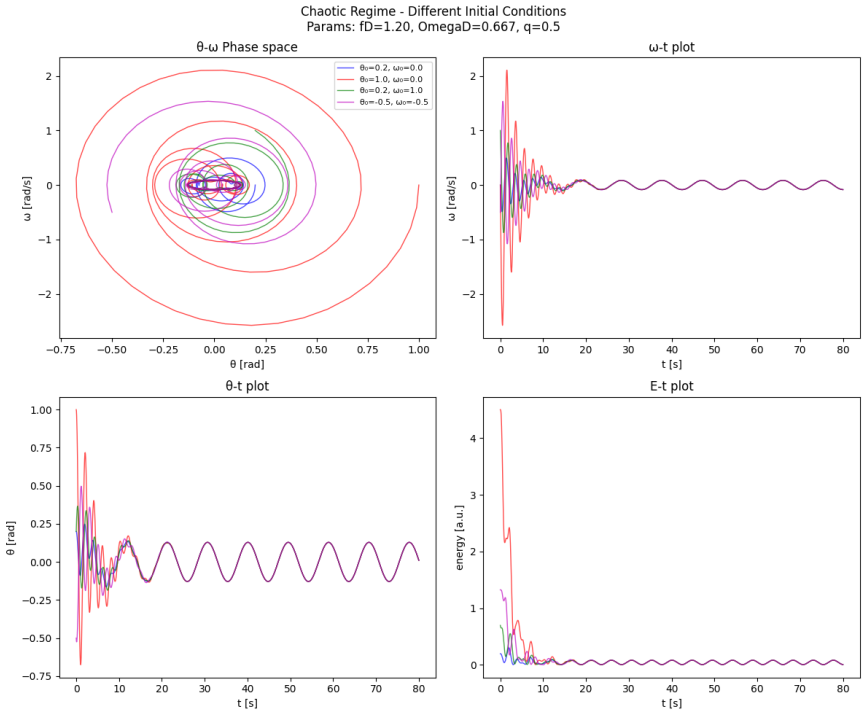

Figure 9: Plots of the phase spaces for the chaotic regime with varied initial conditions.

trajectories eventually fill out the same strange attractor, though they may explore it in different sequences. This suggests that while the motion is chaotic, it is bounded within a well-defined region of phase space.

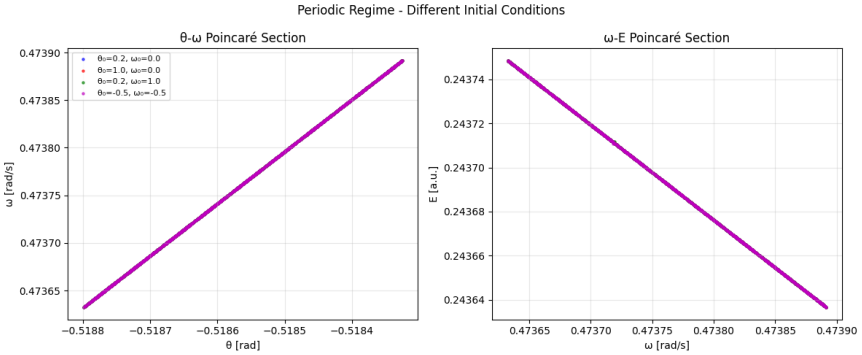

Figure 10: Plot of the Poincare section for the periodic regime with varied initial conditions.

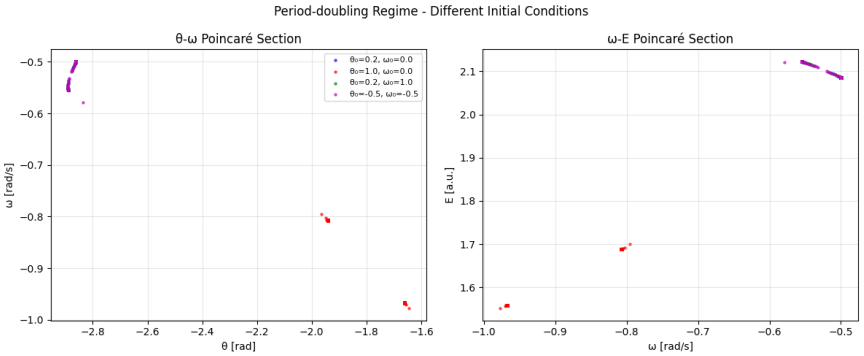

Figure 11: Plot of the Poincare section for the period-doubling regime with varied initial conditions.

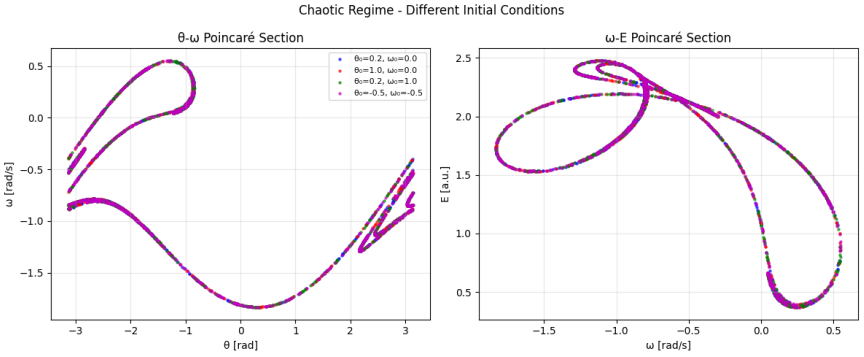

Figure 12: Plot of the Poincare section for the chaotic regime with varied initial conditions.

In all three regimes, the damping term ensures that initial differences eventually disappear, but the time required for this convergence increases as we move from periodic to chaotic behavior. The Poincar sections provide clear evidence that the final state of the system (whether periodic, period-doubled, or chaotic) is determined by the system parameters (F_D, Ω_D, q) rather than the initial conditions, demonstrating the robustness of these dynamical regimes. ■

Problem 3
Third, do the same as in (1) but with changing the phase cut to $\pi/2, \pi$, and 37°. Compare the results with those of parts (1) and (2).

Solution. In this problem, we examine how different phase cuts in the Poincare sections affect our view of the system's dynamics. We compared three different phase cuts: $\pi/2$, π, and 37, while maintaining all other parameters constant for each regime. These phase cuts correspond to sampling the system's state at different points within the driving cycle.

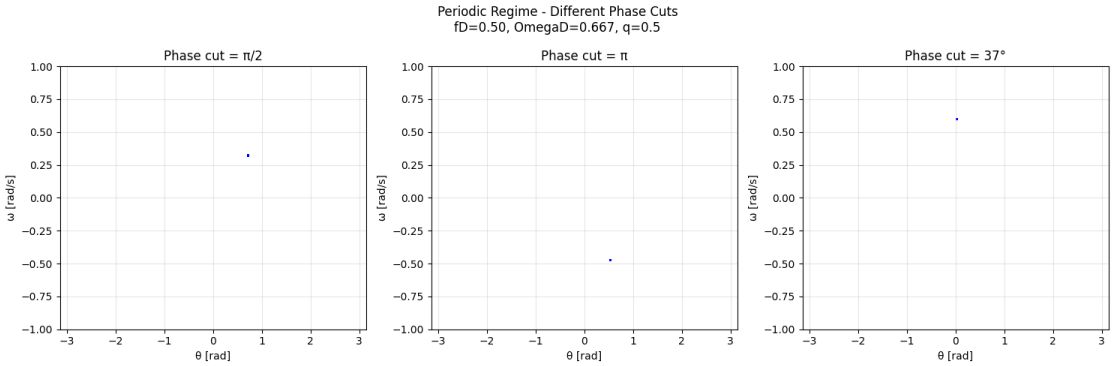

Figure 13: Plots of the phase spaces for the chaotic regime.

In the periodic regime ($F_D = 0.5$), we observe that changing the phase cut simply samples the periodic orbit at different points. Each phase cut shows a single point in the θ-ω space, but at different locations. This is expected since the motion is periodic with the same period as the driving force, so sampling at any fixed phase will always catch the system at the same state, just at different points in its cycle.

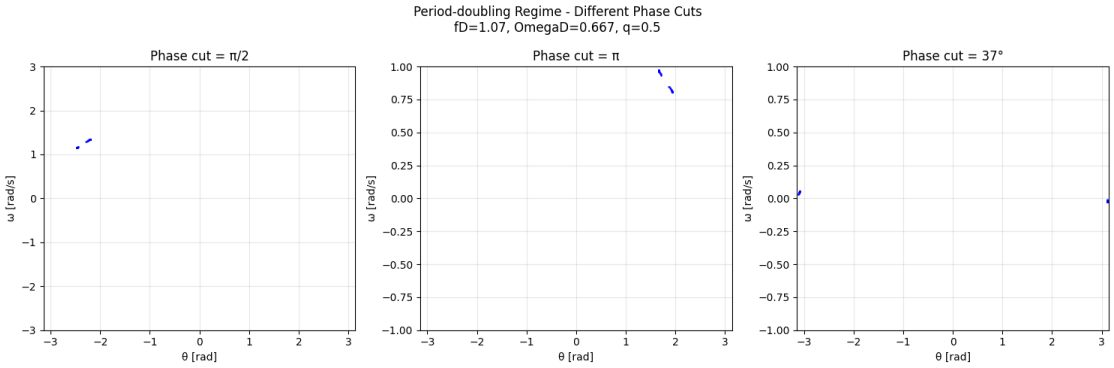

Figure 14: Plots of the phase spaces for the chaotic regime.

For the period-doubling regime ($F_D = 1.07$), each phase cut reveals two distinct points, confirming that the period of the motion is twice that of the driving force. The location of these points varies with the phase cut, but the fundamental period-doubling structure remains intact. This demonstrates that the period-doubling behavior is a robust feature of the dynamics, independent of when we choose to observe the system.
The chaotic regime ($F_D = 1.2$) shows the most interesting variation with phase cut. While all three cuts reveal the chaotic nature of the motion through their scattered point patterns, the structure of these patterns differs notably between cuts. The $\pi/2$ cut shows a more elongated distribution of points, while the π cut reveals a different cross-section of the strange attractor. The 37 cut provides yet another perspective, demonstrating how the strange attractor has a complex structure that appears different depending on where we section it.

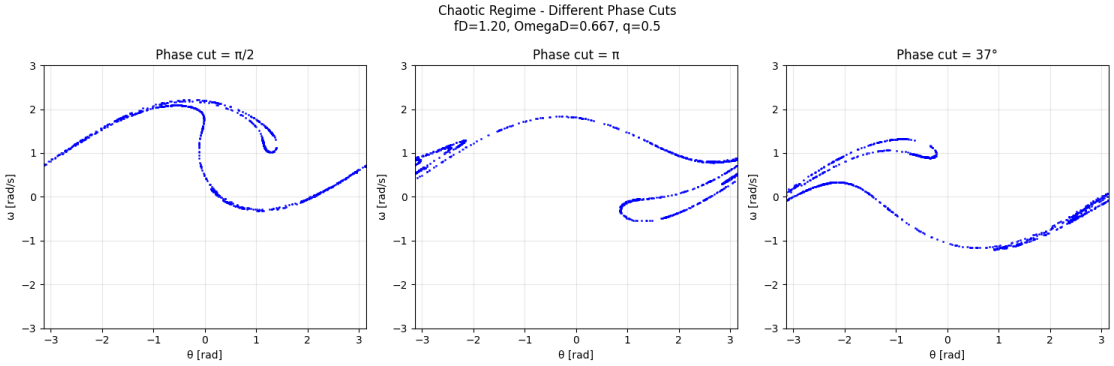

Figure 15: Plots of the phase spaces for the chaotic regime.

These results highlight an important aspect of Poincare sections: while the choice of phase cut affects the specific appearance of the section, the fundamental character of the dynamics (periodic, period-doubled, or chaotic) remains clearly identifiable regardless of the chosen phase. This invariance of the qualitative behavior across different phase cuts confirms that these dynamical regimes are robust features of the system rather than artifacts of our observation method. ■

Problem 4
Lastly, keeping all the other parameters the same as in (1), use an arbitrary sectioning frequency that differs from the driving frequency Ω and is irrationally related to or incommensurate with it. As an example, you can try $\omega_0 = (g/L)^{1/2}$ (the natural angular frequency of the linearized oscillator) or $\omega_1 = (g/L)^{1/2}\pi/\left[2K\left(\sin\left(\theta_m/2\right)\right)\right]$ (that of the nonlinear oscillator without dissipation or driving force, where θ_m is the amplitude). Discuss the results.

Solution. In this final investigation, we examine how the Poincare sections change when using sectioning frequencies that are incommensurate (not rationally related) with the driving frequency. We compared three different frequencies:

- The driving frequency $\Omega = 0.667$ rad/s
- The natural frequency $\omega_0 = \sqrt{g/L} = 1.000$ rad/s
- The golden ratio times the driving frequency $\varphi\Omega \approx 1.079$ rad/s

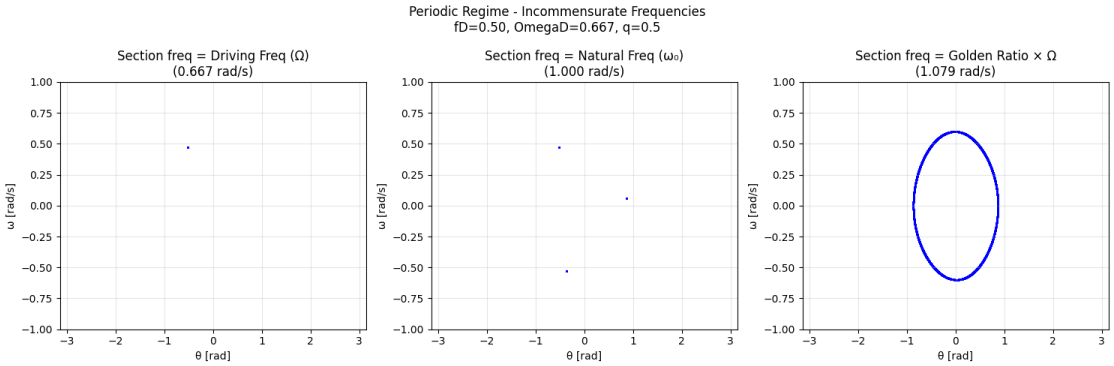

Figure 16: Plots of the phase spaces for the chaotic regime.

For the periodic regime ($F_D = 0.5$), using the driving frequency produces a single point as expected, since we sample the motion at the same phase each period. When using the natural frequency, we see two distinct points, indicating that the system's response includes both driving and natural frequencies. Most interestingly, using the golden ratio frequency produces a closed curve. This occurs because the incommensurate frequency samples the periodic orbit at points that never exactly repeat, eventually filling out the entire trajectory.

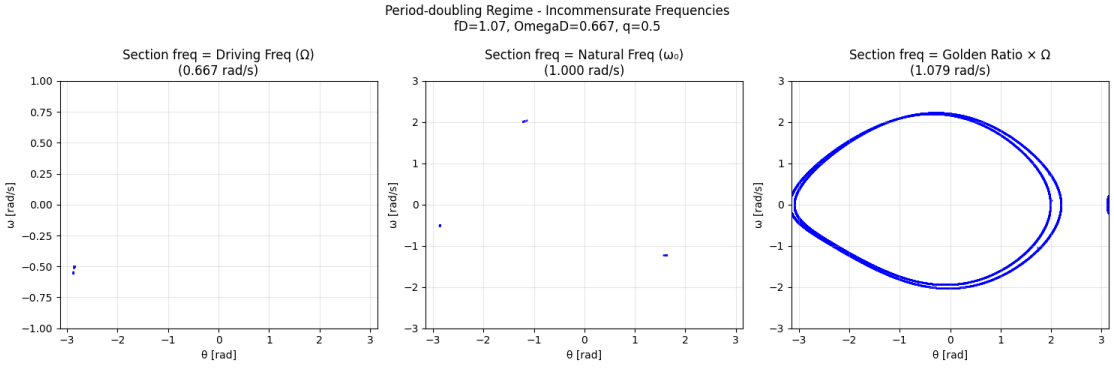

Figure 17: Plots of the phase spaces for the chaotic regime.

In the period-doubling regime ($F_D = 1.07$), the driving frequency reveals the characteristic two-point structure. The natural frequency sampling shows a more complex pattern with multiple points, reflecting the

interplay between the natural, driving, and period-doubled frequencies. The golden ratio frequency again produces a closed curve, but now with a more complex structure that captures the period-doubling nature of the motion.

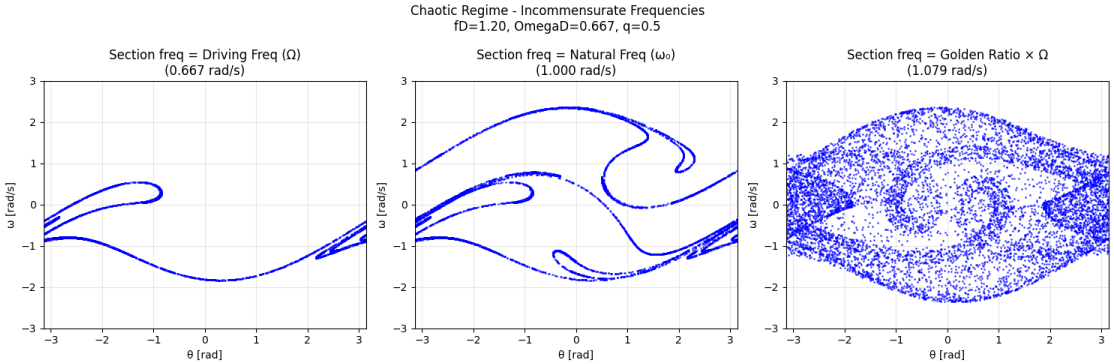

Figure 18: Plots of the phase spaces for the chaotic regime.

The chaotic regime ($F_D = 1.2$) shows the most dramatic differences between sectioning frequencies. The driving frequency produces the now-familiar strange attractor structure. The natural frequency section reveals a similar but distorted pattern, highlighting different aspects of the chaotic attractor. The golden ratio frequency produces an even denser filling of the phase space, as the incommensurate sampling effectively reveals more of the attractor's structure.

These results demonstrate that incommensurate sectioning frequencies can reveal additional structure in the system's dynamics that might not be apparent when using the driving frequency alone. This is particularly evident in the periodic and period-doubling regimes, where incommensurate frequencies transform discrete points into continuous curves. In the chaotic regime, different frequencies provide complementary views of the strange attractor's complex geometry. ■